

## Enhancing Coverage and Rate of Cell Edge User in Multi-Antenna Poisson Voronoi Cells\*

S. Balaji<sup>†</sup>, R. Santhakumar<sup>‡</sup> and P. S. Mallick<sup>§</sup>

*School of Electrical Engineering,  
VIT University, Vellore 632014, India*

<sup>†</sup>*sbalaji@vit.ac.in*

<sup>‡</sup>*santhakumar@vit.ac.in*

<sup>§</sup>*psmallick@vit.ac.in*

Received 10 July 2014

Accepted 4 May 2015

Published 21 July 2015

This paper analyzes the cell edge mobile user performance in the downlink cellular system. We develop frame-work for coverage probability and spectral efficiency. In particular, we analyzed the performance of multi-antenna mobile users under multi-antenna base stations (BSs). The expressions of coverage probability and spectral efficiency are derived for cell edge user using stochastic geometry. We investigate how much the performance of cell edge user is improved when distances connecting BSs and cell edge users are modeled with cell edge null probability distribution. The probability of coverage and spectral efficiency is studied using zero-forcing beam-forming and the performance metrics are compared between coordinated scheduling (CS) and without coordinated scheduling (w/o CS). The interesting observation from our results is that the edge user coverage and rate is closely approaching towards the inner cell typical mobile user's rate and coverage, and the performance is verified with relative probability of coverage gain analysis.

*Keywords:* Coverage probability; spectral efficiency; MIMO; coordinated scheduling; cellular systems.

### 1. Introduction

Existing cellular systems are designed to cater to provide coverage for wider areas and to cope with the high volume of traffic. The data demand from the existing cellular architectures is increasing every day. There are many ingredients in the analysis of cellular network's and their mean values are considered as performance bottlenecks in cellular standards. An essential requirement of the systems is to define and assure good performance of cell edge users with high quality of service (Qos)

\*This paper was recommended by Regional Editor Kshirasagar Naik.

<sup>†</sup>Corresponding author.

metrics.<sup>1</sup> Out of the many, one is explicitly present in providing connection to the users called probability of coverage and the other is related to the spectral efficiency. The network average data rate is analyzed by spectral efficiency which fundamentally relates the spectrum use with growing demands for the service. In Ref. 2, they proved that the Qos plays vital role in cellular optimization, system planning and analysis. The other Qos metric is the diversity gain which is defined as rate of decay of outage probability in the high coverage regime. The diversity gain is studied for heterogeneous joint transmission networks in Ref. 3.

Recent research and communication standards have focused on multi-antenna in base station (BS) and mobile unit (MU) in Ref. 4. The prime objective of multi-antenna communications is to increase the data rates and reliability in cellular communication networks thereby providing good Qos. The multiple-input multiple-output (MIMO) techniques for cellular systems are affected by intercell interference. The intercell interference can be avoided or aligned at the transmitter side and/or removed at the receiver side by way of joint processing. By using the richness of environment one such an alignment technique is developed in Ref. 5. The intercell interference is mitigated by many approaches in the past by way of sharing required information through backhaul. MIMO can take various strategies to cancel out the intercell interference like dirty paper coding (DPC), Eigen beamforming and zero-forcing beamforming, etc. DPC requires the full channel state information at the transmitter side which is difficult to achieve and performs encoding among the users in an ordered manner, and thereby eliminates interference at the transmitter side in Ref. 6. Methodology was also developed to measure the statistical variation of the interference power thereby reducing the interference of networks in Ref. 7. These interference management techniques require joint cooperation among BS and MUs and it is very much limited by backhaul capacity. The difficulty in cooperation and information sharing increases as the network size increases. If the interference is managed in an efficient way, and less the interference, the more will be the coverage probability, spectral efficiency, etc.

In this work, the goal is to maximize the probability of coverage and spectral efficiency of cell edge user and to investigate how multiple antenna enhance the coverage and rate in coordinated scheduling (CS) and without coordinated scheduling (w/o CS) schemes in MIMO downlink environment.

### 1.1. *Related works and contributions*

The major challenges in cellular deployment are the incursion of inter-tier interference and intercell interference due to frequency reuse, which can deteriorate the effectiveness of cellular architecture.<sup>8</sup> Several recent researches have studied MIMO networks with inter-cell and intra-cell interference with variety of BSs deployment. Out of all such abstraction, hexagonal model is most widely applied.

The BS locations are modeled alternatively using a spatial stochastic process namely Poisson point process (PPP) to model the actual BS placements. In most of the models, the signal to interference plus noise ratio (SINR) provided to the user is the basis through which the Qos metrics are measured. Using stochastic geometry tools, the SINR distribution, coverage probability and spectral efficiency in downlink and uplink are characterized by many researchers in the recent past. The calculated values of these parameters by these advanced tools are almost equal to the regular grid model studies.<sup>9</sup> Cellular systems with complex overlay of multiple communication networks are becoming more heterogeneous and variety of infrastructure such as macrocells, picocells, femtocells, etc. have been covered extensively in recent works. In these heterogeneous cells, the downlink coverage probability and area spectral efficiency have been recently studied to a large extent. The performance metrics in downlink are analyzed with varying SINR distribution and cells with different tiers which are biased either to increase the coverage or to increase throughput.<sup>10</sup> The interference is approximated with gamma distributions using stochastic geometry. An interesting observation made in the interference limited heterogeneous networks is that the probability of coverage neither increases nor decreases as one goes on increasing the number of tiers or BSs, see Refs. 11–13 for more details. As said earlier, interference mitigation and coordination techniques are reviewed to a greater extent in the past. Strategies for coding and beam-forming to reduce interference are also reported.<sup>14</sup> Interference is managed with limited feedback mechanism under zero-forcing beam-forming systems and the feedback overhead for interference mitigation and dynamic resource allocation is also studied using stochastic geometry tools.<sup>15,16</sup> The resulting expressions of these geometric models are complex and involve Monte Carlo simulation with multiple random variables.

The work is basically maximizing the performance of cell edge user by canceling the interference and increasing the SINR distribution. To cancel interference, different transmission strategies are proposed. Various transmit antenna schemes with beam-forming or receiver combining techniques are studied by number of researchers either by way of transmission selection schemes or frequency reuse. These methods necessarily increase the transmission capacity and/or system throughput.<sup>17,18</sup> Adaptive strategy was proposed with multiple BS jointly coordinates based on user location<sup>17</sup> and moreover interference management strategy is provided for cell-edge worst-case locations with multi-antennas.<sup>19</sup> The performance of worst-case MUs has also been studied with and without relays in many recent literatures. Worst-case SINR maximization with power control for a multicell environment is developed<sup>20</sup> and analytical expressions for spectral efficiency using scheduling algorithms are derived in Ref. 2. Models for the worst-case MUs are obtained and however these models lack tractability when large number of users are deployed randomly in Refs. 10, 21 and 22. Various forms of scheduling schemes have been reported in recent works to increase the spectral efficiency and the CS schemes for cell edge user are also reported.<sup>23,24</sup>

The performance evaluation of inner cell (typical) MU is analyzed in Refs. 9, 11 and 24 for single input single output (SISO) systems and also coverage, rate and capacity of MUs are characterized in multi-antenna environments.<sup>15,18,19,25–27</sup> In almost all of these models, they utilized the inner cell probability density function (PDF) for distances between MUs and BSs. Specifically in any of these recent works, they have not quantified the performance evaluation of cell edge or worst-case MUs in multi-antenna configuration with null probability distribution of worst-case MUs. These recent studies do not guarantee the worst-case MUs about their communication rate or their area coverage from BSs. This shortcomings motivate our work to develop a mathematical treatment for worst-case MUs to decide their rate or coverage. Basically, our innovation in this work is the study of cell edge user coverage probability and spectral efficiency with CS and w/o CS in multi-antenna system and to the best of our knowledge, this is the first such approach for worst-case MUs. Since the MUs are worst-case MUs, we invoked worst-case MU null PDF for distances connecting MUs and BSs from Ref. 28. Our contributions are summarized below.

In our CS analysis, we scheduled the edge cell or worst-case MU which is placed at a point where the distances to nearby neighboring cells are almost equal. To simplify the analysis, in our work, we modeled the worst-case MU was nearer to three nearest BSs and the performance metrics are studied by deriving the suitable expressions. It can also be extended to more general framework. Performance metric comparison is made to make our system study interesting i.e., performance metric comparison here is made with multiple receive and multiple serving BS antennas and the new thing in this work is the study of performance variation of probability of coverage and spectral efficiency in Poisson Voronoi cells cell edge user with a cell edge probability distribution function (PDF) which is different from inner cell PDF. Specifically, the probability of coverage and spectral efficiency are derived for different cases in such a way that each case comes form whether number of receive antennas (MU) are greater than or equal to the number of transmit antennas (BS). In each of the case, the effectiveness of neighboring (interfering) BS antennas on coverage and spectral efficiency of worst-case MU is evaluated in order to study the effects of interference on MU when the number of antennas of MU is changing. We derived the probability of coverage expression for the edge cell or worst-case mobile user by considering interference coming from multi-antenna BSs and each BS takes different transmission strategies.<sup>17</sup> We also studied the coverage probability when BS powers are varying and we obtained more coverage for lower ratio of transmits powers of BSs. The analytical expressions for spectral efficiency are obtained for coordinated and uncoordinated scheduling scheme. The numerically computed value of the spectral efficiency for coordinated and uncoordinated scheduling schemes are compared and analyzed with varying antenna numbers. The obtained results are matching with the existing standard results and are comparatively better than other reported works.

The rest of the paper is organized as follows. The system model is introduced in Sec. 2 and the expressions for probability of coverage are derived in Sec. 3 and in

Sec. 4, the probability of coverage is extended for CS. Spectral efficiency of cell edge user is discussed in Sec. 5. Numerical results and comparisons are presented in Sec. 6 which corroborates the analytical derivations. Finally, Sec. 7 concludes the paper.

## 2. System Model

In classical cellular model, BSs are placed at the centers of hexagonal cells and the intercell and intracell interference are investigated in a fixed cell from many tiers of interferers. In stochastic geometry cellular systems, MUs and BSs follow PPP and our detailed system model is described below.

The downlink cellular system is considered and it's assumed to be consisting of BSs and MUs. The mobiles are modeled by a homogeneous PPP  $\Phi$  of density  $\lambda$ . Regular cell models assume channel powers from BSs are constant and do not differentiate between cell edge and interior users. Moreover BSs are all independent in the Euclidean plane and MUs are scattered about the plane. Each mobile user is attached to the nearest BSs resulting in better areas of coverage that encompass a Voronoi Tessellation. If the MU is connected to the nearest BS, the region around the BS is divided as voronoi cells and such regions are termed as Poisson voronoi tessellation. One such tessellation with BSs at the centre and mobiles distribution is shown in Fig. 1.

In Fig. 1, the MU at point A is surrounded by four BSs and brings more complexity in interference management. At point B, the MU is nearer to three BSs. The MUs at points A and B are called edge cell MUs or worst-case MU. The mobile at

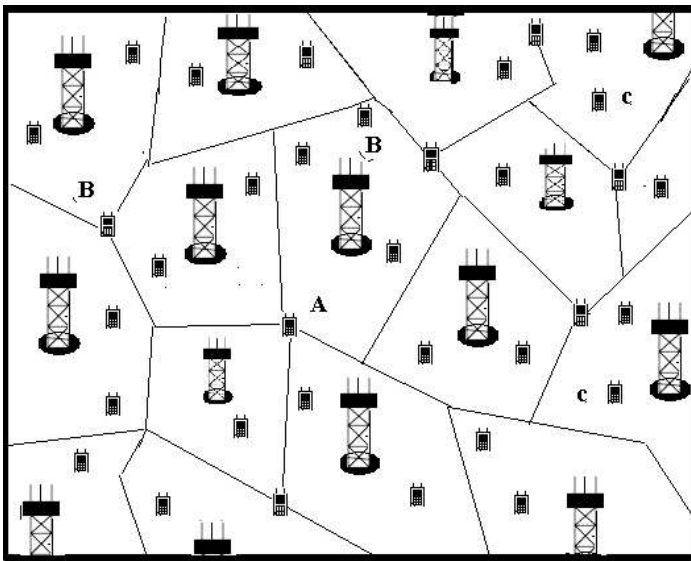


Fig. 1. Poisson Voronoi Tessellations of MUs and BSs.

C receives strong signal from one of the BS and it is termed as inner cell MU. The BSs are assumed to be having  $N_t$  antennas and the MUs are equipped with  $N_r$  antennas. The desired signal power from the serving station BS is termed as  $P_i$  and the interference from the  $j$ th neighboring BS is represented as  $P_j$ . The sum of all  $P_j$  is written as  $P_x$ . For General framework, we consider  $P_i$  and  $P_j$  are set to unity and hence each antenna transmit power is equal to  $1/N_t$ . In this work,  $W$  represents the additive white gaussian noise and the standard path loss model is assumed and the path loss  $L(x) = \|X\|^{-\alpha}$  and the value of path loss exponent  $\alpha > 2$ . The fading vector  $N_t \times 1$  between the  $q$ th antenna of the BS  $\in \Phi$  and the MU is denoted by  $h_{x,q} \sim \text{CN}(0_{N_t \times 1}, I_{N_t})$ .

Each BS uses its  $N_\omega$  antennas to transmit independent streams to  $M$  users in its own cell where  $M$  is less than or equal to  $N_\omega$ . If  $M$  is less than  $N_\omega$ , the remaining  $N_t - N_\omega$  antennas are used for either doing intercell interference cancellation (ICIC) in neighboring cells or to cater to the new users arising from the same cell and/or migrating from other cells. In our model, the number of receive antennas  $N_r$  can be made equal to  $k + N_t$  i.e.,  $N_r = k + N_t$  and  $k = N_r - N_t$ . The  $N_r$  antennas at the MU is used to cancel the intracell interference cancellation or ICIC or to enhance the desired signal strength. The number of receive antennas  $N_r$  in MU is now a function of  $k$  and by suitably taking various values for  $k$ , the effectiveness of the proposed methodology is demonstrated for coverage probability and spectral efficiency. The serving BS for the MU is denoted by  $b_0$  and the other BSs situated around the BS  $b_0$  is denoted by  $b_1, b_2$  and so on. The MU present in  $b_0$  is assumed to be interested in decoding the  $k$ th transmitted stream  $a_{b_0,k}$  from serving BS  $b_0$ . Thus the  $N_r \times 1$  signal received at the MU from  $b_0$  is written in Ref. 25 as:

$$y_k = \frac{P_0 a_{b_0,k}}{\sqrt{r^\alpha}} h_{b_0,k} + \frac{P_0}{\sqrt{r^\alpha}} \sum_{q=1, q \neq k}^{N_t} h_{b_0,q} a_{b_0,k} + I(\Phi) + W, \tag{1}$$

where

$$I(\Phi) = \sum_{x \in \{\Phi/b_0\}} \frac{P_x}{\sqrt{\|x\|^\alpha}} \sum_{q=1, q \neq k}^{N_t} h_{x,q} a_{x,q}.$$

The  $I(\Phi)$  defines the intercell interference from all other BSs other than  $b_0$ . This is the cumulative interference seen by the MU when it is attached to the tagged BS  $b_0$ .

### 2.1. SINR in zero-forcing beamforming

In order to characterize the distribution of signal and interference, we evaluated the SINR with a zero-forcing beamforming in our system. The SINR distribution can also be studied using other methods like minimum mean square error (MMSE), ordered successive interference cancellation methods<sup>29</sup> and so on and the zero-forcing

beamforming receiver is simple to implement and yields a near optimal performance. Now we describe the beamforming methodology adopted in our model.

The downlink beamforming is focused on zero-forcing beamforming and in the beamforming vector  $w_{b_0,q}$  is the unit norm beamforming vector for the MU in  $b_0$ . If the MU in  $b_0$  is decoding the signal from  $b_0$ , the unit norm precoding vector  $w$  is chosen as orthogonal to the following vectors<sup>25</sup>

$$h_{b_0,q} : q = 1, 2, 3, \dots, k-1, k+1, \dots, N_t,$$

$h_{x,q} : x = \{b_0, b_1, \dots, b_{n-1}\}$  and where  $\{b_0, b_1, \dots, b_{n-1}\}$  are the closest BSs around the MU. From our system model, if the MU is assumed to be resided in  $b_0$ , the received signal at MU can be written as

$$\check{y}_k = \frac{a_{b_0,k}}{\sqrt{r^\alpha}} w^\dagger h_{b_0,k} + \frac{1}{\sqrt{r^\alpha}} \sum_{q=1, q \neq k}^{N_t} w^\dagger h_{b_0,q} a_{b_0,k} + w^\dagger I(\Phi) + w^\dagger W. \quad (2)$$

Let us define  $G_0 = |w^\dagger h_{b_0,k}|^2$  and  $H_{x,q} = |w^\dagger h_{x,q}|^2$ . The zero-forcing SINR at the worst-case MU is represented as

$$\text{SINR}_\zeta = \frac{P_0 G_0 r^{-\alpha}}{N_t \sigma^2 + I(\Phi)}, \quad (3)$$

where

$$I(\Phi) = P_1 G_1 r^{-\alpha} + P_2 G_2 r^{-\alpha} + \sum_{x \in \{b_0, b_1, b_1\}} P_x \|x\|^{-\alpha} \sum_{q=1}^{N_t} H_{x,q}.$$

While writing the expression (3), the inter-stream interference is neglected, since the MU's will be having minimum of  $N_r = N_t$  antennas to cancel it. In most of the multi-antenna techniques, the desired signal and interfering signal power are considered to be gamma distributed.<sup>16</sup> In our system, the number of users  $M$  reaches to the value of  $N_\omega$ , then the desired signal power is distributed as  $\Gamma(N_t - N_\omega + 1, 1)$ . This model is equivalent to SDMA. If  $N_\omega$  is equivalent one, and the model reduces to MISO with single user beamforming and the signal is  $\Gamma(N_t, 1)$ . If  $N_r$  antennas are used to receive the desired signal at the MU, the received signal is distributed as  $\Gamma(N_r - N_t + 1, 1)$  and the model becomes MIMO. From above discussions, the signal power of the desired received signal  $|w^\dagger h_{b_0,k}|^2$  is to be maximized.

The beamforming vector is designed in such a way that the received signal at each user is a chi square random variable and the number of degrees of freedom comes from whether the system uses ICIC using zero-forcing beamforming or simple beamforming (SF). Thus

$$|w^\dagger h_{b_0,k}|^2 = \begin{cases} \chi_{2N_t} & \text{SF} \\ \chi_{2N_t-m} & \text{ICIC} \end{cases}.$$

From the above equation, if the BS does the ICIC for neighboring cells instead of doing self fish beamforming, the signal power distribution reduces by  $N_t - m$  where  $m$  is the set of cardinality i.e., number of other cells where it does ICIC.<sup>17</sup> Similarly if the neighboring cells use SF, the interference signal at the MU is identically independently distributed exponential and their sum is gamma distributed. Suppose if neighboring cells perform ICIC, the interference power distribution is reduced. In our model, each BS has  $N_t$  antennas, so the interference is distributed as  $\Gamma(N_t, 1/N_t)$ . The worst-case MU is in coverage if one of the SINR from the serving BSs is greater than the target threshold.

### 2.2. Base station distances

The BS distances are vital parameters in the derivation of coverage probability. Since MUs are in communication with the serving BSs, there are two distances  $R$  and  $r$ . The distance  $R$  is the distance of interference from the MU and  $r$  is the separating distance between the serving BS and the worst-case MU. The PDF of  $r$  from the palm distribution of PPP is expressed as

$$f_r(r) = \frac{dF_r}{dr}$$

and the null probability is defined in our case is

$$\begin{aligned} P[r > R] &= P[\text{No BS closer than } R] \\ &= (1 + \lambda\pi r^2)e^{-\pi r^2}. \end{aligned} \tag{4}$$

Therefore, worst-case or cell edge user probability distribution function from Ref. 24 is  $f_r(r) = 2(\pi\lambda)^2 r^3 e^{-\pi r^2}$ . This distribution function is different from the inner cell probability distribution function which is expressed in Ref. 9 as  $2(\pi\lambda)re^{-\pi r^2}$ . In the next section, the probability of coverage is analyzed for the cell edge MU.

### 3. Probability of Coverage

The probability of coverage of w/o CS can be considered as the cell edge MU's SINR being greater than the target threshold  $\theta$  or equivalently average fractions of users who achieve target SINR greater than  $\theta$  at any time. From probability theory, it is nothing but the complementary cumulative distribution function (CCDF) of SINR in the network. The probability of coverage is defined as

$$p_c(k, N_t, \theta) = P[\text{SINR} > \theta]. \tag{5}$$

From the above equation, the cell edge MU is in coverage if its SINR is higher than the threshold  $\theta$  from its nearest BSs.

We first derive the general expression for probability of coverage of w/o CS for cell edge MU's. Since the probability of coverage is SINR greater than some

threshold  $T$ , first the signal strength received on  $k$  antennas will need to be evaluated. From our system model, the received signal strength is distributed as  $\Gamma(N_r - N_t + 1, 1)$  because  $k = N_r - N_t$ . Next the Laplace transform of interference emanating from neighboring (interfering) BSs with  $N_t$  antennas conditioned on the BS distances  $R$  and  $r$  is evaluated to find SINR when worst-case MU has  $k$  antennas. The consequence of coverage probability for various values of  $k$  is presented as a special case.

**Proposition 1.** *The probability of coverage of MU located in cellular network is upper bounded by*

$$p_c(k, N_t, \theta) = \sum_{k=0}^{N_r-N_t} \frac{1}{k!} \int_{r>0} (-\theta)^k \frac{\partial^k}{\partial \theta^k} \{2(\pi\lambda)^2 r^3 e^{-\theta N_t \sigma^2 - \pi R^2 \lambda * 2F1(N_t, -\frac{2}{\alpha}, \frac{\alpha-2}{\alpha}, -P_x R^{-\alpha} \theta)}\} dr. \quad (6)$$

**Proof.** The MU is located in one of the cellular networks and is associated with one of the BSs which is at  $r$  distance away, the probability of coverage is

$$\begin{aligned} p_c(k, N_t, \theta) &= E_r[P[\text{SINR} > T | r]], \\ p_c(k, N_t, \theta) &= E_r \left[ P \left[ \frac{P_0 G_0 r^{-\alpha}}{N_t \sigma^2 + I(\Phi)} > T | r \right] \right], \\ p_c(k, N_t, \theta) &= E_r \left[ P \left[ G_0 > T \frac{(N_t \sigma^2 + I(\Phi))}{P_0 r^{-\alpha}} | r \right] \right]. \end{aligned} \quad (7)$$

Now we evaluate the probability

$$P \left[ G_0 > \frac{(N_t \sigma^2 + I(\Phi))}{P_0 r^{-\alpha}} | r \right]$$

as

$$\begin{aligned} &P \left[ G_0 > \frac{T(N_t \sigma^2 + I(\Phi))}{P_0 r^{-\alpha}} | r \right] \\ &\stackrel{(a)}{=} E_{I_r} \left[ e^{-(TP_0^{-1} r^\alpha (N_t \sigma^2 + I(\Phi)))} \sum_{k=0}^{N_r-N_t} \frac{(TP_0^{-1} r^\alpha (N_t \sigma^2 + I(\Phi)))^k}{k!} | I_r \right], \end{aligned} \quad (8)$$

where the equality (a) follows from CCDF of  $G_0$  i.e.,  $G_0 = \Gamma(N_r - N_t + 1, 1)$  The number of MU antennas  $k$  in terms of transmit BS antennas  $N_t$  varies from  $k = 0$  to  $k = \infty$  and it is an important parameter through which we derive expressions for coverage probability and spectral efficiency of our proposed model in coordinated and uncoordinated schemes. Since the distribution is gamma, and if we take the first summation  $k = 0$ , then the number of antennas  $N_r - N_t + 1$  will be equal to 1 i.e.,  $N_r - N_t + 1 = 1$ , and if  $N_r - N_t + 1 = 2$ , it equals to  $k = 1$  (second summation) and so on. Sec. 3.1 for detailed derivation for various values of  $k$ .

Now denote  $\theta$  as  $TP_0^{-1}r^\alpha$ ,  $I_r$  as  $I(\Phi)$ , and substitute Eq. (8) in Eq. (7). The probability of coverage at a distance  $r$  is evaluated as

$$\begin{aligned}
 p_c(k, N_t, \theta) &\stackrel{(a)}{=} \int_r E_{I_r} \left[ e^{-(\theta(N_t\sigma^2 + I(\Phi)))} \sum_{k=0}^{N_r - N_t} \frac{(\theta I_r)^k}{k!} \right] f_r(r) dr, \\
 p_c(k, N_t, \theta) &= \int_r \sum_{k=0}^{N_r - N_t} \frac{1}{k!} e^{-\theta N_t \sigma^2} E_{I_r} [e^{-(\theta I_r)} (\theta I_r)^k] f_r(r) dr, \\
 E_{I_r} [e^{-(\theta I_r)} (\theta I_r)^k] &\stackrel{(b)}{=} (\theta)^k \{t^k f_{I_r}(t)\}(\theta), \\
 E_{I_r} [e^{-(\theta I_r)} (\theta I_r)^k] &\stackrel{(c)}{=} (-\theta)^k \frac{\partial^k}{\partial \theta^k} L_{I_r}(\theta),
 \end{aligned} \tag{9}$$

where the equality (a) holds when the noise power

$$\frac{1}{\sigma^2} \rightarrow \infty, (\theta(N_t\sigma^2 + I(\Phi)))^k \rightarrow (\theta I_r)^k,$$

and while making the equality, the probability of coverage is averaged over the plane conditioning on the nearest BS at  $r$ . The equality (b) follows from the definition of Laplace transform and the equality (c) follows from the differentiation identity of the Laplace transform

$$t^n f(t) = (-1)^n \frac{\partial^n}{\partial s^n} \{L(f(t))\}(s)$$

Thus the Eq. (9) becomes,

$$p_c(k, N_t, \theta) = \int_r \sum_{k=0}^{N_r - N_t} \frac{1}{k!} e^{-\theta N_t \sigma^2} (-\theta)^k \frac{\partial^k}{\partial \theta^k} L_{I_r}(\theta) f_r(r) dr. \tag{10}$$

The  $L_{I_r}(\theta)$  is derived in [Appendix A](#).

Substituting the value of  $L_{I_r}(\theta)$  from Eq. (A.2) in the above Eq. (10) completes the derivation of **Proposition 1**. From **Proposition 1**, the probability of coverage of w/o CS can be computed for worst-case MU. The term  $2F1(a, b, c, z)$  is the regularized hypergeometric function.<sup>30</sup>  $\square$

### 3.1. Special cases of without coordinated scheduling

The probability of coverage in **Proposition 1** is a function of number of antennas  $k$ . The values of  $k$  i.e., the number of antennas which contribute to the probability of coverage in **Proposition 1** are considered here as special cases. These special cases helps in finding whether increasing the additional MU antennas  $k$  from one to many really boosts the probability of coverage or not. These additional antennas  $k$  can be used to enhance signal strength or to cancel the intercell interference. To simplify the coverage analysis, the noise is taken as zero and the system becomes interference

limited system. In interference limited system, the noise power is negligible ( $\frac{1}{\sigma^2} \rightarrow \infty$ ). The interference limited system can be applied for various transmit and receive antenna configurations and here in our analysis probability of coverage is expressed for two special cases. The results of the special cases with respect to each interfering antenna  $N_t$  are plotted in Sec. 6 and compared against the recently published works.<sup>27</sup>

**Case 1.** If we set  $k = 0$ , it corresponds to the number of receiving antennas of MU i.e.,  $N_r = N_t$  of the serving BS. In this case, the summation of the probability of coverage is not necessary. The probability of coverage is reduced to computable form as

$$p_c(0, N_t, \theta) = \int_0^\infty 2(\pi\lambda)^2 r^3 e^{-\pi R^2 \lambda * 2F1(N_t, -\frac{2}{\alpha}, \frac{\alpha-2}{\alpha}; -P_x R^{-\alpha} \theta)} dr. \quad (11)$$

If the mobile is in edge i.e.,  $r = R$  and each BS transmits a constant power and it is set to unity, then the coverage probability after substituting the value of  $\theta$  reduces to

$$p_c(0, N_t, T) = \frac{1}{2F1[N_t, -\frac{2}{\alpha}, \frac{-2+\alpha}{\alpha}, -T]^2}. \quad (12)$$

Notice that the above coverage probability is independent of the density of BSs. Interesting observation made from the above expression is that this coverage probability of worst-case MU is lower than the probability of coverage of inner cell MU<sup>3</sup> (typical) which is varying as  $\frac{1}{2F1[N_t, -\frac{2}{\alpha}, \frac{-2+\alpha}{\alpha}, -T]}$ . But we could obtain worst-case coverage probability equivalently better than inner cell coverage by incorporating CS which is discussed in detailed manner in Sec. 4.

**Case 2.** The choice of  $k = 1$  corresponds to  $N_r = N_t + 1$  antennas of serving BS. For this configuration, the coverage probability is evaluated by differentiating the interference with respect to the threshold  $\theta$  and substituting the result of the differentiation in Eq. (6). Thus, the coverage probability reduces to the computable form as

$$p_c(1, N_t, \theta) = \int_{r>0} (-\theta) \frac{\partial}{\partial \theta} \{2(\pi\lambda)^2 r^3 e^{-\pi R^2 \lambda * 2F1(N_t, -\frac{2}{\alpha}, \frac{\alpha-2}{\alpha}; -P_x R^{-\alpha} \theta)}\} dr + p_c(0, N_t, T).$$

The first derivative of interference is

$$\begin{aligned} & \frac{\partial}{\partial \theta} \left\{ e^{-\pi R^2 \lambda * 2F1(N_t, -\frac{2}{\alpha}, \frac{\alpha-2}{\alpha}; -\theta)} \right\} \\ &= e^{-\pi R^2 \lambda * 2F1[N_t, -\frac{2}{\alpha}, \frac{-2+\alpha}{\alpha}, -\theta]} \\ & \times \left( \frac{2}{\alpha \theta} * \pi R^2 \lambda \left\{ (1 + \theta)^{-N_t} - 2F1 \left[ N_t, -\frac{2}{\alpha}, \frac{-2 + \alpha}{\alpha}, -\theta \right] \right\} \right). \end{aligned}$$

After substituting the above equation in the previous equation and integrating the resulting expression, the coverage probability becomes

$$p_c(1, N_t, T) = \frac{\left(-4(1+T)^{-N_t} + 4 * 2F1\left[N_t, -\frac{2}{\alpha}, \frac{-2+\alpha}{\alpha}, -T\right]\right) + \alpha\left(2F1\left[N_t, -\frac{2}{\alpha}, \frac{-2+\alpha}{\alpha}, -T\right]\right)}{\alpha\left(2F1\left[N_t, -\frac{2}{\alpha}, \frac{-2+\alpha}{\alpha}, -T\right]^3\right)}. \quad (13)$$

Likewise, the coverage can be expressed for many numerous worst-case MU's antennas in terms of serving BS antennas. We have also plotted the results for  $k = 2$  and final expression for  $k = 2$  is given as Eq. (D.1) in Appendix D. As the number of antennas increases, the complexity of the expression grows and also the computation is difficult. This can be evaluated numerically using Faà di Bruno's formula and can be expanded using Bell's polynomial.

### 3.2. Coverage with varying transmit power

In complex overlay of networks, transmit powers, traffic load carrying capability and radio environment are all different. These networks are often completely random in nature and deployed irregularly as an overlay of severe dense networks with limited coverage and rate. Mostly in these networks, transmit power across different tiers is different and their ratio may not be equal to unity in most of the networks. To support greater cell edge user rate and coverage in these networks, the probability of coverage with respect to the desired signal power  $P_i$  and interference power  $P_x$  which is coming from all neighboring BSs having  $N_t$  antennas are necessary. To derive the coverage probability analysis with BSs of varying transmit powers, we slightly keep the ratio of desired signal power to the interference power as greater than unity i.e.,  $\delta = \frac{P_i}{P_x} \geq 1$ . This methodology can be well approximated to heterogeneous networks. The following lemma aids in understanding the coverage probability of edge cell MU when it is served by BSs of different transmit powers.

**Corollary 1.** *The probability of coverage of MU when BS powers are not equal is*

$$p_c(k, N_t, T, \delta) = \left(\frac{\delta}{\delta + T}\right)^{2N_t} \left\{ \frac{1}{2F1\left[N_t, -\frac{2}{\alpha}, \frac{-2+\alpha}{\alpha}, -\frac{T}{\delta}\right]^2} \right\}. \quad (14)$$

The above lemma (**Corollary 1**) is derived for  $k = 0$  i.e., the MU's receive antennas  $N_r$  will be equal to the desired BS antennas  $N_t$ . It can be extended to different values of  $k$  and it is left for future work. The above **Corollary 1** is plotted for different  $N_t$  and the plot is shown in Sec. 6.

**Proof.** See **Appendix B**. □

#### 4. Coverage in Coordinated Scheduling

One of the best schemes to mitigate ICI is the CS scheme. The CS scheme can easily be implemented in practice via limited feedback. It aims at making the system operate at desired point on the ergodic achievable rate region of the system.<sup>31</sup> The scheduling policy handles the MUs with different CSI Levels and allocates the signaling modes opportunistically. Practically the rate maximizing scheduler offers good compromise in system gain by selecting MUs with high received powers.

Since each BS exchanges information such as CQI and CDI, the BS which has the best channel conditions to the worst-case MU connects to the MU in a given allocated time or subframe to guarantee the performance of MU. To simplify the analysis, we consider the MU is located at a typical point where three BSs are almost equidistant away.

If BSs exchange information through backhaul and coordinate in serving the MUs, the effects of such coordination on probability of coverage is to be known to find whether the coordination is really increasing the coverage or not. To substantiate that the coordination is really enhances the coverage, the coverage probability in CS for different antenna schemes is derived in this section.

**Proposition 2.** *The probability of coverage of the cell edge MU under CS scheme is*

$$\begin{aligned}
 p_{CS}(k, N_t, \theta) = & \int_r \sum_{k=0}^{N_r - N_t} \frac{1}{k!} e^{-\theta N_t \sigma^2} (-\theta)^k \frac{\partial^k}{\partial \theta^k} \left[ 2e^{-\lambda * R^2 * \pi * \Psi(N_t, -\nu)} - e^{-\lambda * R^2 * \pi * \Psi(N_t, -2\nu)} \right. \\
 & + \left. \left\{ e^{-\lambda * R^2 * \pi * \Psi(N_t, -2\nu)} - 2e^{-\lambda * R^2 * \pi * \Psi(N_t, -\nu)} + e^{-\lambda * R^2 * \pi} \left( \frac{\Gamma[N_t, \theta N_t]}{\Gamma[N_t]} \right) \right\} \right] \\
 & \times 2(\pi\lambda)^2 r^3 dr, \tag{15}
 \end{aligned}$$

where

$$\Psi(N_t, -\nu) = 2F1 \left[ -\frac{2}{\alpha}, N_t, \frac{-2 + \alpha}{\alpha}, -\nu \right] \quad \text{and} \quad \nu = \frac{T}{N_t}.$$

Compared with uncoordinated scheduling, the coverage probability obtained in Eq. (15) is better.

**Proof.** In CS, the MU chooses one of the BSs whose signal strength is maximum of the three signal strengths and the worst-case MU is exactly equidistant away from three BSs. Here, one of the BS uses simple beamforming to ensure continuous communication of MU, and other BSs serve the users with  $N_t$  antennas. Thus, the interfering power  $G_i$  from all interfering BSs are identically independently exponential with mean  $1/N_t$ . Moreover in our CS scheme, as already said, one of the BS uses simple beamforming, and thus the desired signal power  $G_i$  from one BS is gamma distributed there-by making the channel of the desired BS independent of everything. The probability of coverage of the edge cell MU when it is nearer to three

BSs<sup>24</sup> is computed as

$$\int_{r>0} P \left[ \frac{\max(G_0, G_1, G_2)r^{-\alpha}}{I(\Phi)} > \theta \mid r \right] f_r(r) dr.$$

$$p_{cs}(k, N_t, \theta) = \int_r \sum_{k=0}^{N_r-N_t} \frac{1}{k!} e^{-\theta N_t \sigma^2} E_{I_r} \left[ \left( \frac{e^{-\frac{2r-\alpha\theta}{N_t}} ((-1 + 2e^{\frac{r-\alpha\theta}{N_t}}) \Gamma[N_t] + (-1 + e^{\frac{r-\alpha\theta}{N_t}})^2 \Gamma[N_t, r^{-\alpha} \theta N_t])}{\Gamma[N_t]} \right) (\theta I_r)^k \right] \times f_r(r) dr. \tag{16}$$

Equation (16) is derived after following the similar procedure used in deriving Eq. (8) i.e., taking the complementary cumulative distribution function of desired signal and applying here maximum SINR probability criterion.

$$E_{I_r} \left[ \left( \frac{e^{-\frac{2r-\alpha\theta}{N_t}} ((-1 + 2e^{\frac{r-\alpha\theta}{N_t}}) \Gamma[N_t] + (-1 + e^{\frac{r-\alpha\theta}{N_t}})^2 \Gamma[N_t, r^{-\alpha} \theta N_t])}{\Gamma[N_t]} \right) (\theta I_r)^k \right] = (-\theta)^k \frac{\partial^k}{\partial \theta^k} \left\{ -L_{I_{rCS}} \left( \frac{-2\theta}{N_t} \right) + 2L_{I_{rCS}} \left( \frac{-\theta}{N_t} \right) + \left\{ L_{I_{rCS}} \left( \frac{-2\theta}{N_t} \right) - 2L_{I_{rCS}} \left( \frac{-\theta}{N_t} \right) + L_{I_{rCS}} \left( \frac{0}{N_t} \right) \right\} \left( \frac{\Gamma[N_t, \theta N_t]}{\Gamma[N_t]} \right) \right\}.$$

Taking the expectation and applying probability generating functional as explained in the equations from Eqs. (A.1) to (A.2) and evaluating at  $r = R$ , the Laplace transform of total interference when Interfering BSs have  $N_t$  antennas becomes

$$\left\{ -L_{I_{rCS}} \left( \frac{-2\theta}{N_t} \right) + 2L_{I_{rCS}} \left( \frac{-\theta}{N_t} \right) + \left\{ L_{I_{rCS}} \left( \frac{-2\theta}{N_t} \right) - 2L_{I_{rCS}} \left( \frac{-\theta}{N_t} \right) + L_{I_{rCS}} \left( \frac{0}{N_t} \right) \right\} \left( \frac{\Gamma[N_t, \theta N_t]}{\Gamma[N_t]} \right) \right\} = \left\{ 2e^{-\lambda * R^{2*\pi} * 2F1[N_t, -\frac{2}{\alpha}, \frac{-2+\alpha}{\alpha}, (\theta)]} - e^{-\lambda * R^{2*\pi} * 2F1[N_t, -\frac{2}{\alpha}, \frac{-2+\alpha}{\alpha}, ((-2*\theta))]} + \left\{ e^{-\lambda * R^{2*\pi} * 2F1[N_t, -\frac{2}{\alpha}, \frac{-2+\alpha}{\alpha}, (-2*\theta)]} - 2e^{-\lambda * R^{2*\pi} * 2F1[N_t, -\frac{2}{\alpha}, \frac{-2+\alpha}{\alpha}, (-\theta)]} + e^{-\lambda * R^{2*\pi}} \right\} \left( \frac{\Gamma[N_t, \theta N_t]}{\Gamma[N_t]} \right) \right\}.$$

Putting the above equation in Eq. (16), we obtain the desired result. Now by changing the desired antenna value  $k$ , the following special cases are derived for CS.

□

**4.1. Special cases in coordinated scheduling**

The impact of number of antennas on the probability of coverage in CS is derived in this section and **Proposition 2** necessitates the arrival of special cases. The special cases are very necessary since the coverage of CS derived in **Proposition 2** is also a function of number of antennas. The derived expressions in CS for different antenna combinations provide a good probability of coverage for worst-case MU and it achieves a better coverage as that of inner cell MU.

**Case 1.** By making  $k = 0$ , the number of receiving antennas  $N_r$  will be equal to  $N_t$  of the serving BSs and as said earlier, if  $k = 0$  the summation of the probability of coverage is not necessary. The probability of coverage in CS reduces to

$$\begin{aligned}
 p_{c_{CS}}(0, N_t, \theta) = & \int_r \left[ 2e^{-\lambda * R^2 * \pi * \Psi(N_t, -\nu)} - e^{-\lambda * R^2 * \pi * \Psi(N_t, -2\nu)} \right. \\
 & + \left. \left\{ [e^{-\lambda * R^2 * \pi * \Psi(N_t, -2\nu)} - 2e^{-\lambda * R^2 * \pi * \Psi(N_t, -\nu)} + e^{-\lambda * R^2 * \pi}] \right. \right. \\
 & \left. \left. \times \left( \frac{\Gamma[N_t, \theta N_t]}{\Gamma[N_t]} \right) \right\} \right] 2(\pi\lambda)^2 r^3 dr.
 \end{aligned}$$

After algebraic manipulations and integrating the above equation and substituting the value of  $\theta$  yields the coverage probability as

$$\begin{aligned}
 p_{c_{CS}}(0, N_t, T) & \\
 & = \frac{\Gamma[N_t, TN_t] \left( 1 + \frac{1}{2F1 \left[ -\frac{2}{\alpha}, N_t, \frac{-2+\alpha}{\alpha}, -\frac{2T}{N_t} \right]^2} - \frac{2}{2F1 \left[ -\frac{2}{\alpha}, N_t, \frac{-2+\alpha}{\alpha}, -\frac{T}{N_t} \right]^2} \right)}{\Gamma[N_t]} \\
 & + \frac{2}{2F1 \left[ -\frac{2}{\alpha}, N_t, \frac{-2+\alpha}{\alpha}, -\frac{T}{N_t} \right]^2} - \frac{1}{2F1 \left[ -\frac{2}{\alpha}, N_t, \frac{-2+\alpha}{\alpha}, -\frac{2T}{N_t} \right]^2}. \quad (17)
 \end{aligned}$$

If we compare the coverage of w/o CS given in Eq. (12) with this probability of coverage, there are additional hypergeometric functions in Eq. (17). These additional terms are necessarily coming out from probability distribution of maximum SINR among three coordinating BSs and from null probability distribution of BS distances connecting the worst-case MU. This additional hypergeometric functions contribute to better probability of coverage. Instead, if MU connects only to one BS whose SINR is either maximum or minimum, there will not be any additional terms to contribute better probability of coverage. If MU is connected like this, then the coverage probability of CS will reduce to without CS scheme. Similar argument holds good for other special cases in CS scheme as well.

**Case 2.** By adopting the similar procedure outlined in case 2 of Sec. 3.1, the probability of coverage in the CS is derived as

$$p_{CCS}(1, N_t, \theta) = \int_{r>0} (-\theta) \frac{\partial}{\partial \theta} \{2(\pi\lambda)^2 r^3 L_{I_{rCS}}(\theta)\} dr + p_{CCS}(0, N_t, T).$$

The first derivative of interference is

$$\begin{aligned} \frac{\partial}{\partial \theta} \{L_{I_{rCS}}(\theta)\} &= \frac{1}{\Gamma[N_t]} \Gamma[N_t, \theta N_t] \left( -\frac{1}{\alpha\theta} 4 * \Delta(-\theta) * \Delta'(-\theta) \right. \\ &\quad \left. + \frac{1}{\alpha\theta} 2\Delta(-2\theta)\Delta'(-2\theta) \right) \\ &\quad + \frac{1}{\alpha\theta} 4\Delta(-\theta)\Delta'(-\theta) - \frac{1}{\alpha\theta} 2\Delta(-2\theta)\Delta'(-2\theta) \\ &\quad - \frac{1}{\Gamma[N_t]} e^{-\theta N_t} \{e^{-\pi R^2 \lambda} + \Delta(-2\theta) - 2\Delta(-\theta)\} N_t (\theta N_t)^{-1+N_t}, \quad (18) \end{aligned}$$

where

$$\begin{aligned} \Delta(-\theta) &= \text{Exp}\left(-\pi R^2 \lambda 2F1\left[-\frac{2}{\alpha}, N_t, \frac{-2+\alpha}{\alpha}, -\frac{\theta}{N_t}\right]\right) \quad \text{and} \\ \Delta'(-\theta) &= \pi R^2 \lambda \left(-2F1\left[-\frac{2}{\alpha}, N_t, \frac{-2+\alpha}{\alpha}, -\frac{\theta}{N_t}\right] + \left(1 + \frac{\theta}{N_t}\right)^{-N_t}\right). \end{aligned}$$

Substituting the above Eq. (18) in the previous equation  $p_{CCS}(1, N_t, \theta)$  and integrating, completes the coverage probability for  $k = 1$  configuration and is given by

$$p_{CCS}(1, N_t, T) = \frac{1}{\alpha\Gamma[N_t]} \left[ \frac{4(\Gamma[N_t] - \Gamma[N_t, TN_t]) \left(1 + \frac{2T}{N_t}\right)^{-N_t}}{\Psi(N_t, -2\nu)^3} - \frac{4\Gamma[N_t] - 4\Gamma[N_t, TN_t] - e^{-TN_t} \alpha (TN_t)^{N_t}}{\Psi(N_t, -2\nu)^2} \right. \\ \left. \left\{ \Gamma[N_t] \left(8 * \Psi(N_t, -\nu) - 8 \left(1 + \frac{T}{N_t}\right)^{-N_t}\right) + \Gamma[N_t, TN_t] \left(-8 * \Psi(N_t, -\nu) + 8 \left(1 + \frac{T}{N_t}\right)^{-N_t}\right) + e^{-TN_t} \alpha * \Psi(N_t, -\nu) (-2 + \Psi(N_t, -\nu)^2) (TN_t)^{N_t} \right\} \right. \\ \left. + \frac{\Psi(N_t, -\nu)^3}{\Psi(N_t, -\nu)^3} \right], \quad (19)$$

where  $\Psi(N_t, -\nu)$  is already defined in Proposition 2. The coverage probability results are plotted for the above cases in addition to the other choice where  $k = 2$ . The necessary expression for  $k = 2$  is given in Appendix D as Eq. (D.2) without detailed derivation.

### 5. Spectral Efficiency

This section deals with the spectral efficiency of worst-case MU with and w/o CS. This is the average rate obtainable over a cell. Specifically for cell edge user, we quantify the achievable rate in units of nats/Hz so that naturally each user decides on its rate it wants to communicate. It is interesting to see that our derived spectral efficiency in multi-antenna configuration with worst-case MU probability distribution is much higher than the SISO or typical MU which uses inner cell PDF. While deriving the expression for spectral efficiency, the interference is taken as noise. The spectral efficiency is defined as in Ref. 24 as

$$\tau = E[\ln(1 + \text{SINR})],$$

$$\tau(k, N_t) = \int_{t>0} \int_{r>0} P \left[ \ln \left( 1 + \frac{P_0 G_0 r^{-\alpha}}{N_t \sigma^2 + I(\Phi)} \right) > t \right] f_r(r) dr dt,$$

where  $P_0$  is taken as unity and  $\sigma^2 = 0$ .

From Theorem 2 of Ref. 25, the inner integral is the probability of coverage at a given distance  $r$ . By taking the inner integral as probability of coverage, the spectral efficiency is written as

$$\tau(k, N_t) = \int_{t>0} p_c(k, N_t, \theta) dt.$$

Substituting Eq. (12) in the above equation and evaluating at the threshold, the spectral efficiency of uncoordinated scheduling scheme is

$$\tau(0, N_t) = \int_{t>0} \frac{1}{2F1 \left[ N_t, -\frac{2}{\alpha}, \frac{-2 + \alpha}{\alpha}, -(e^t - 1) \right]^2} dt. \tag{20}$$

By using this, we can numerically compute the spectral efficiency of without coordination scheme for different MUs and interfering antenna configurations. By adopting the similar procedure, the spectral efficiency can be computed for various values of  $k$  against various  $N_t$ .

**Spectral Efficiency in CS:** The spectral efficiency of the CS schemes is derived for various values of  $k$  as

**Corollary 2.** *The spectral efficiency of the CS of edge MU is*

$$\tau_{cs}(0, N_t) = \frac{\Gamma[N_t, \nu(t)] \left( 1 + \frac{1}{\Psi(N_t, -2\nu)^2} - \frac{1}{\Psi(N_t, -\nu)^2} \right)}{\Gamma[N_t]} + \frac{2}{\Psi(N_t, -\nu)^2} - \frac{1}{\Psi(N_t, -2\nu)^2}, \tag{21}$$

where

$$\Psi(N_t, -\nu(t)) = 2F1 \left[ -\frac{2}{\alpha}, N_t, \frac{-2 + \alpha}{\alpha}, -\nu(t) \right] \quad \text{and} \quad \nu(t) = \frac{e^t - 1}{N_t}.$$

The spectral efficiency is computed numerically from **Corollary 2** for different values of  $N_t$  and the efficiency performance of edge cell MU is discussed in Sec. 6. Working out on the similar lines, separate expressions can be derived for different  $k$  values.

**Proof.** See **Appendix C**. □

## 6. Numerical Results

In this section, we have analyzed the numerical results for the probability of coverage and spectral efficiency with and w/o CS. The random Poisson model is well suited to model the actual BS placements and MUs in cellular systems. All the derived expressions are independent of density of BSs. In all our simulations, we take the standard value for the path loss which is usually between  $\alpha = 2$  and  $\alpha = 4$  and in our simulation it is taken as  $\alpha = 4$  and the noise is taken to be zero and the values of the simulation parameters are given in Table 1.

### 6.1. Probability of coverage comparison

Figure 2 compares the probability of coverage for  $k = 0$  ( $N_r = N_t$ ) between CS and uncoordinated scheduling. The key observation from the plot is that as the number of BS antennas  $N_t$  increases the number of receive antennas  $N_r$  will also increase by the same quantity since  $N_r = N_t$ . Increasing  $N_r$  is not only increasing the coverage but helps in canceling the interference which comes from equal number of  $N_t$  antennas of interfering BSs. Moreover, increasing  $N_t$  in BSs increases the interference from neighboring BSs also at MU. Because of this increased interference distribution, the coverage probability decreases. Observe that probability of coverage of  $N_t = 1$  is higher than the  $N_t = 2$  and  $N_t = 2$  is higher than  $N_t = 3$ . This clearly demonstrates that as  $N_t$  increases, coverage decreases.

Table 1. Simulation parameters.

Parameter	Value
$\alpha$	4
$k$	0,1,2
$N_t$	1,2,3
$\sigma^2$	0
$T$	-5 dB to 15 dB
$\delta$	20

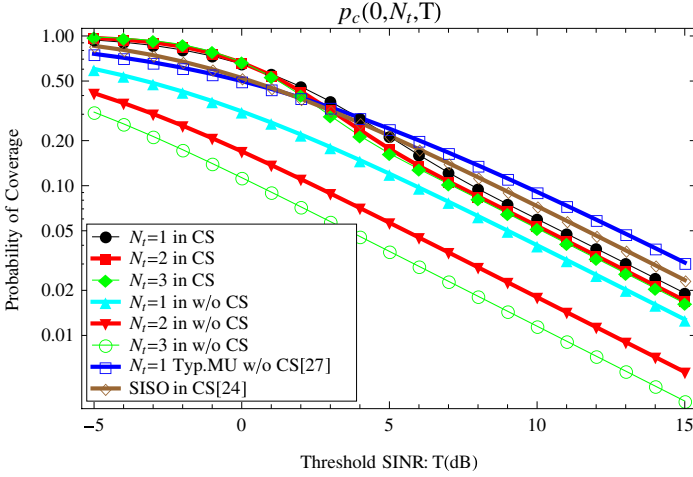


Fig. 2. Probability of coverage of worst-case MU when  $k = 0$ .

Instead, if the MU is coordinated based on the maximum signal gain it receives from the BSs around it, the received desired signal strength will be higher. Hence, the probability of coverage is expected to increase. The plot also clearly demarcates the increase in the probability of coverage when MU is in CS. Notice similar configuration of  $N_t$  in CS is having higher probability of coverage than without CS. Our edge user CS coverage is higher than the SISO of Ref. 24 at lower thresholds but at higher thresholds, because of strong interference, it is slightly lower. The coordination scheduling probability is comparatively higher than the typical MU obtained in Ref. 27. One can easily observe from the plot that the cell edge user coverage of this approach is comparatively having very good coverage with CS.

The probability of coverage is compared between CS and uncoordinated scheduling for the special cases  $k = 1$  ( $N_r = N_t + 1$ ) and  $k = 2$  ( $N_r = N_t + 2$ ) in Figs. 3 and 4. The useful insight from the plots is that the system can select the best combinations of antennas to increase the probability of coverage. By increasing  $k$ , the proposed method really aids in desired signal enhancement i.e.,  $k$  increases the probability of coverage increases. As already said, one can infer from the plots that the MU probability is less compared to the scheduling scheme and it goes on decreasing if the number of interfering BS antennas  $N_t$  increases like  $N_t = 1$ ,  $N_t = 2$  and so on. This inference comes from the fact that the number of antennas in the MU increases, the coverage probability is increased and the increase in the coverage probability is more significant, if the system chooses the CS scheme. The significant increase in coverage probability is observed in Fig. 4 and the probability slightly reduces, if the interfering BS antennas increases. Moreover, typical MU is also plotted against this for easy analysis. There is a slight edge effect observed in Fig. 3 at higher threshold in CS and similar edge effect is also reported in Refs. 11 and 26.

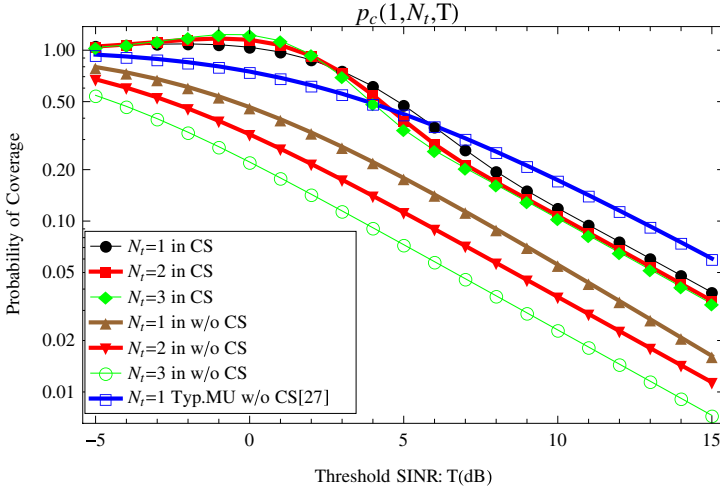


Fig. 3. Probability of coverage of worst-case MU when  $k = 1$ .

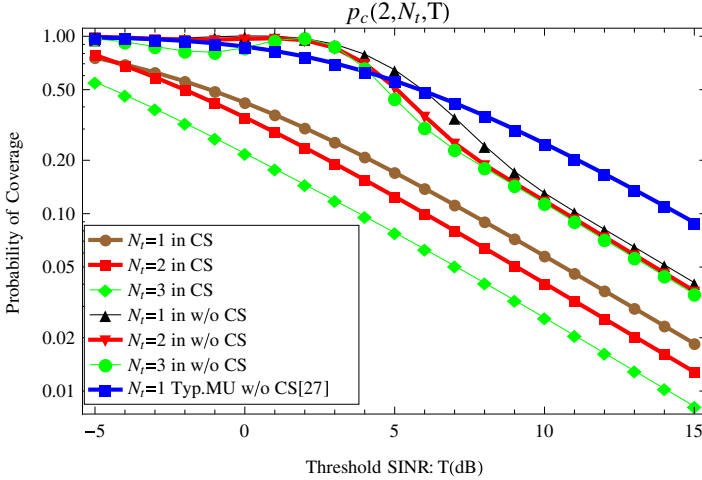


Fig. 4. Probability of coverage of worst-case MU when  $k = 2$ .

Figure 5 compares the probability of coverage for BSs when their powers are varying. From Fig. 5, one can easily observe that our proposed methodology produces very high coverage even if the ratio of desired signal power to interfering power is very minimum. As the number of transmitting antennas increases, we expect the transmitted powers to be shared between the antennas thereby keeping the power budget constant. From the plot, the model clearly shows that as the number of  $N_t$

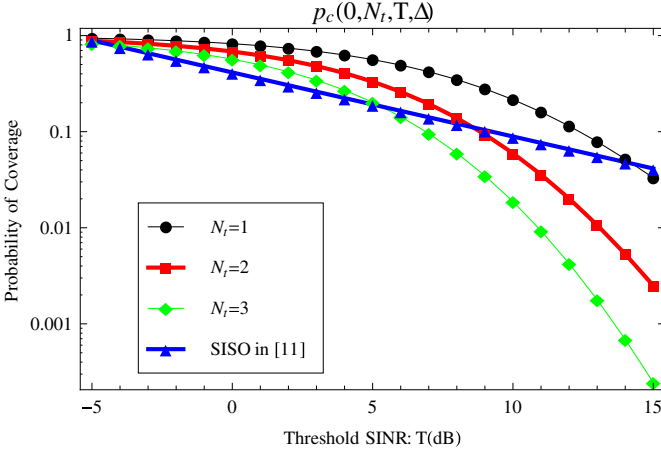


Fig. 5. Probability of coverage when powers of BS's varying ( $k=0$  and  $\delta=20$ ).

antennas increases, the power required to meet the probability of coverage also increases. The observed results are in very good match with SISO network reported in Ref. 11. This varying power model can be used to obtain the coverage probability when the MU is choosing between different networks of cells. It can also be plotted easily for different values of MU antenna configurations.

### 6.2. Effect of antennas on spectral efficiency

The spectral efficiency is also computed numerically for various transmit and receive antenna combinations and is given in Table 2. While computing the spectral efficiency, we have taken 1 bit = 0.693 nats. As the number of interfering BS antennas  $N_t$  increases, the expected spectral efficiency of cell edge user decreases if  $k$  is kept constant. This is due to increased interference from neighboring BSs. Instead if  $k$  increases and interfering antennas  $N_t$  remains constant, then the spectral efficiency increases. As  $k$  increases, the MU uses additional antennas to communicate with BS, there by increasing its spectral efficiency.

In Ref. 24, they computed a spectral efficiency of 0.39 Bps/Hz and we achieved a result of 0.940 Bps/Hz for the same antenna configurations and our model has clearly made a marked improvement in cell edge MU spectral efficiency. Moreover this spectral efficiency is 43% of that of the MU (typical) obtained in recent work.<sup>9</sup> By applying CS scheme, the achievable spectral efficiency compared to typical MU in Ref. 9 is 71%. In comparison with edge MU in Ref. 24, the proposed method shows better improvement.

The decrease in spectral efficiency is not more pronounced in CS i.e., as interference increases, less decrease in spectral efficiency is observed on our model. Thus,

Table 2. Spectral efficiency in Bps/Hz.

Scheme	Spectral efficiency	Number of interfering BS antennas ( $N_t$ )		
		$N_t = 1$	$N_t = 2$	$N_t = 3$
w/o CS	$\tau(0, N_t)$	0.940 > {0.39 in Ref. 24}	0.593	0.447
	$\tau(1, N_t)$	1.480	0.972	0.748
	$\tau(2, N_t)$	2.376	1.64	1.33
CS	$\tau_{cs}(0, N_t)$	1.546 > {1.49 in Ref. 24}	1.508	1.498
	$\tau_{cs}(1, N_t)$	2.38	2.15	2.01
	$\tau_{cs}(2, N_t)$	2.94	2.72	2.58

clearly from Table 2, the CS scheme achieves higher spectral efficiency with more MU antennas and results are compared with respect to Ref. 24.

Thus increasing  $N_t$ , increases the number of streams and thereby reducing the network performance.

### 6.3. Rate and probability gain

The transmission rate i.e., average ergodic rate can be directly equated to the probability of coverage. If the capacity achieving codebooks are available and from Eq. (5), the bandwidth normalized communication rate from the cooperating BSs to the MU can be expressed as  $R = \ln(1 + \theta)$ . By substituting  $e^R - 1$  in place of threshold  $T$  in Eqs. (12), (13), (17) and (19), equating the resulting expression to the probability of coverage  $p_c$ , and solving for  $R$ , the behavior of probability of coverage with respect to rate  $R^3$  can be studied for without coordination and CS schemes. The variation of probability of coverage against rate is plotted in Figs. 6 and 7. It is very

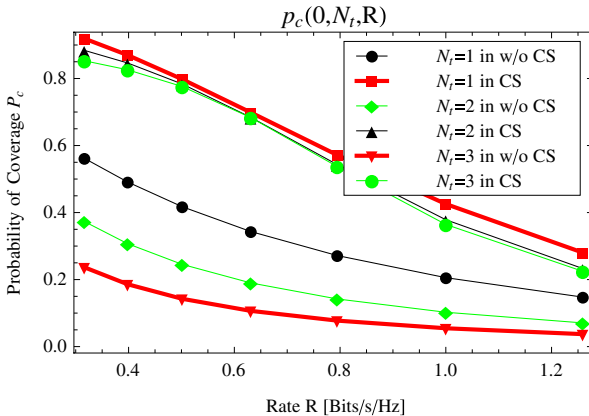


Fig. 6. Probability of coverage of worst-case MU (with CS and w/o CS) when  $k = 0$ .

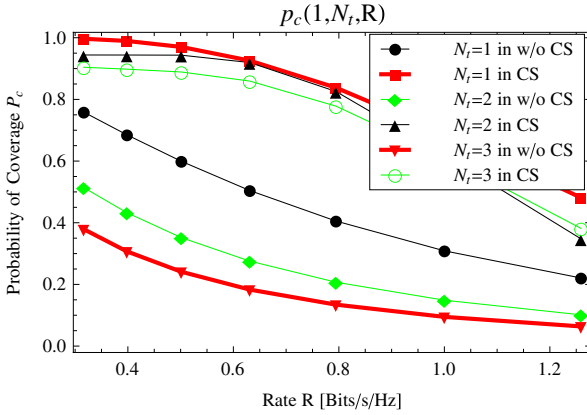


Fig. 7. Probability of coverage of worst-case MU (with CS and w/o CS) when  $k = 1$ .

clear from plots 6 and 7, the probability of coverage in the CS is higher compared to the without coordination. Moreover from the plot, if higher rate is required, the probability to provide such a rate is low and if the number of interfering antennas  $N_t$  increases, the coverage decreases.

Figures 8 and 9 illustrate the variation of relative probability of coverage gain in terms of attainable rate  $R$  for the choices of  $k = 0$  and  $k = 1$ . The relative probability

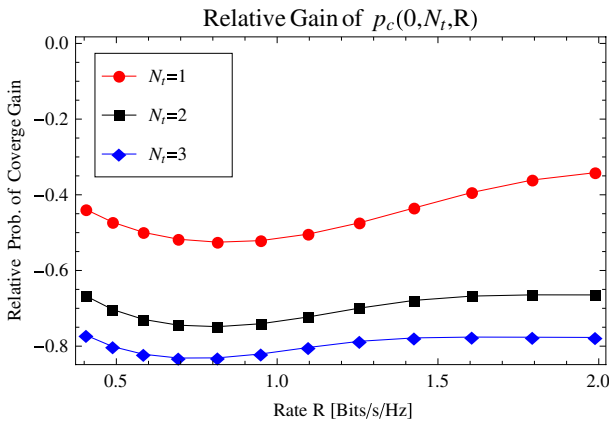


Fig. 8. Relative probability of coverage gain of worst-case MU when  $k = 0$ .

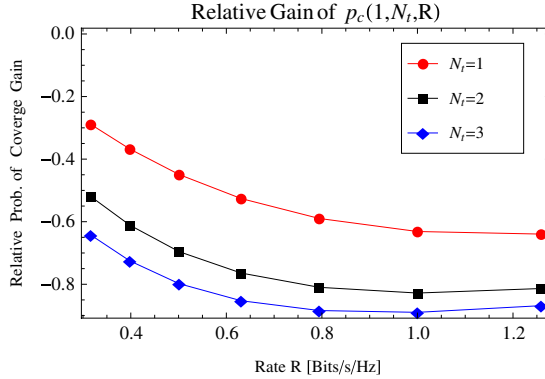


Fig. 9. Relative probability of coverage gain of worst-case MU when  $k = 1$ .

gain is computed as

$$\frac{p_c(k, N_t)(R) - p_{cs}(k, N_t)(R)}{p_{cs}(k, N_t)(R)}, \tag{22}$$

where  $p_c(k, N_t)(R)$  represents the probability of coverage w/o CS at given rate  $R$  and  $p_{cs}(k, N_t)(R)$  the probability of coverage with CS at a rate  $R$ . Notice that in Figs. 8 and 9, the probability gain is negative and it indicates that to achieve the same rate as that of CS, the system should provide a higher probability of coverage i.e., in Fig. 8, around 40% of more probability is required with an interfering antenna of  $N_t = 1$  to catch up the probability of coverage of CS. If we compare the Figs. 8 and 9, one can observe that as the number of MU antennas increases above  $N_t$  i.e.,  $k$  increases, gain required to meet the rate as equal to CS decreases.

Relative probability of coverage gain can be extended for other values of  $k$ . Thus, our average ergodic rate and probability of coverage gain clearly explains our improvement in the performance measure of spectral efficiency.

### 7. Conclusion

We presented the downlink cellular system cell edge user analysis. The performance of cell edge MU is analyzed with multi-antenna combinations employing zero-forcing beamforming under CS and uncoordinated scheduling schemes. We proved that performance metrics in CS under multiple transmit and interfering antenna combinations with edge cell null probability distribution was better than w/o CS counterparts. Our methodology shows an increase in spectral efficiency and coverage probability of cell edge MU compared to existing methods and the improvement is verified by relative probability gain analysis. It can be easily extended to other forms

of transmitter and receiver beamforming. Further extension to this work is to explore how the various forms of fading affect the edge user.

### Appendix A

The Laplace transform of the interference when interfering BSs have  $N_t$  antennas and transmit with a power  $P_x$  is evaluated as  $L_{I_r}(\theta)$

$$L_{I_r}(\theta) = \mathbb{E}[e^{-\theta I_r}] = \mathbb{E} \exp \left[ -\theta \sum_{x \in \Phi} P_x \|x\|^{-\alpha} \sum_{q=1}^{N_t} H_{x,q} \right] \quad (\text{A.1})$$

$$L_{I_r}(\theta) = \mathbb{E}[e^{-\theta I_r}] = \mathbb{E} \prod_{x \in \Phi} \exp \left[ -\theta P_x \|x\|^{-\alpha} \sum_{q=1}^{N_t} H_{x,q} \right] = \mathbb{E} \prod_{x \in \Phi} \frac{1}{(1 + \theta P_x \|x\|^{-\alpha})^{N_t}}$$

$$\begin{aligned} &\stackrel{(a)}{=} \exp(-2\pi\lambda \int_R^\infty \left( 1 - \frac{1}{(1 + \theta P_x \|x\|^{-\alpha})^{N_t}} \right) x dx \\ &= \exp(-\pi R^2 \lambda \left( 2F1 \left( N_t, -\frac{2}{\alpha}; \frac{\alpha - 2}{\alpha}; -P_x R^{-\alpha} \theta \right) - 1 \right)). \end{aligned} \quad (\text{A.2})$$

The equality (a) follows for probability generating functional.<sup>1</sup> Substituting the above equation in Eq. (10) and averaging out using nearest neighbor distribution of Ref. 32 will complete the proof. The above obtained expression is more or less similar to the one obtained in Ref. 25 but because of the transmit powers of BSs and MUs, the interference power will have a different scaling. Moreover, here it is analyzed with multi-antenna gamma distributed desired signal between the PPP BSs and the MUs.

### Appendix B

The Laplace transform of interference if the BSs powers are varying is expressed as

$$L_{I_r}(\theta) = \mathbb{E}[e^{-\theta I_r}] = \mathbb{E} \exp \left[ -\theta \sum_{x \in \Phi} P_x \|x\|^{-\alpha} \sum_{q=1}^{N_t} H_{x,q} \right], \quad (\text{B.1})$$

$$L_{I_r}(\theta) = \mathbb{E}[e^{-\theta I_r}] = \mathbb{E} \prod_{x \in \Phi} \exp \left[ -\theta P_x \|x\|^{-\alpha} \sum_{q=1}^{N_t} H_{x,q} \right]$$

$$\begin{aligned} &\stackrel{(a)}{=} \frac{1}{(1 + \theta P_x \|x\|^{-\alpha})^{2N_t}} \mathbb{E} \prod_{x \in \Phi} \frac{1}{(1 + \theta P_x \|x\|^{-\alpha})^{N_t}} \\ &\stackrel{(b)}{=} \frac{1}{(1 + \theta P_x \|x\|^{-\alpha})^{2N_t}} \exp(-2\pi\lambda \int_R^\infty \left( 1 - \frac{1}{(1 + \theta P_x \|x\|^{-\alpha})^{N_t}} \right) x dx \end{aligned}$$

$$\begin{aligned}
 &= \frac{1}{(1 + \theta P_x x^{-\alpha})^{2N_t}} \exp \left( -\pi R^2 \lambda \left( 2F1 \left( N_t, -\frac{2}{\alpha}; \frac{\alpha - 2}{\alpha}; -P_x R^{-\alpha} \theta \right) - 1 \right) \right) \\
 &\stackrel{(c)}{=} \frac{2(\pi \lambda)^{2r^3}}{(1 + \theta P_x x^{-\alpha})^{2N_t}} \exp \left( -\pi R^2 \lambda \left( 2F1 \left( N_t, -\frac{2}{\alpha}; \frac{\alpha - 2}{\alpha}; -P_x R^{-\alpha} \theta \right) \right) \right). \quad (B.2)
 \end{aligned}$$

The equality (a) is from Rayleigh fading assumptions, (b) follows for probability generating functional and (c) is from Eq. (13) of Ref. 24. After substituting the value of  $\theta$  and taking  $\delta = P_i/p_x$ , Eq. (B.2) is substituted in Eq. (10) and integrating the resulting expression will yield the result.

### Appendix C

The spectral efficiency is obtained in the CS by taking one of the BSs use simple beamforming and other two BSs serves  $N_t$  users. The spectral efficiency is

$$\tau_{cs}(k, N_t) = \int_{t>0} \int_{r>0} P \left[ \ln \left( 1 + \frac{\max[P_0 G_0 r^{-\alpha}, P_1 G_1 r^{-\alpha}, P_2 G_2 r^{-\alpha}]}{N_t \sigma^2 + I(\Phi)} \right) > t \right] f_r(r) dr dt. \quad (C.1)$$

Suppose if the system is interference limited i.e.,  $\sigma^2 = 0$  and assume all the BSs transmit with equal powers ( $P = 1$ ), then the inner term in the above Eq. (C.1) is simplified as

$$\begin{aligned}
 &P[\max(G_0, G_1, G_2) > (I(\Phi)(e^t - 1))] \\
 &= \left\{ -L_{I_r} \left( \frac{2}{N_t} (e^t - 1) \right) + 2L_{I_r} \left( \frac{1}{N_t} (e^t - 1) \right) \right\} * \Gamma[N_t] \\
 &\quad + \left\{ L_{I_r} \left( \frac{2}{N_t} (e^t - 1) \right) - 2L_{I_r} \left( \frac{1}{N_t} (e^t - 1) \right) + L_{I_r}(0) \right\} * \Gamma[N_t, (e^t - 1)N_t]
 \end{aligned}$$

Following the similar steps used in the derivation of Eq. (16) and after some algebraic manipulations the spectral efficiency is derived as

$$\begin{aligned}
 &\tau_{cs}(0, N_t) \\
 &= \int_{t>0} \left\{ \frac{\Gamma[N_t, (e^t - 1)N_t] \left( 1 + \frac{1}{2F1 \left[ -\frac{2}{\alpha}, N_t, \frac{-2+\alpha}{\alpha}, -\frac{2(e^t-1)}{N_t} \right]^2} - \frac{2}{2F1 \left[ -\frac{2}{\alpha}, N_t, \frac{-2+\alpha}{\alpha}, -\frac{(e^t-1)}{N_t} \right]^2} \right)}{\Gamma[N_t]} \right. \\
 &\quad \left. + \frac{2}{2F1 \left[ -\frac{2}{\alpha}, N_t, \frac{-2+\alpha}{\alpha}, -\frac{(e^t-1)}{N_t} \right]^2} - \frac{1}{2F1 \left[ -\frac{2}{\alpha}, N_t, \frac{-2+\alpha}{\alpha}, -\frac{2(e^t-1)}{N_t} \right]^2} \right\} dt. \quad (C.2)
 \end{aligned}$$

**Appendix D.**

**D.1. Probability of coverage of without coordinated scheduling**

The equation for  $k = 2$  when edge MU is in coverage is given by

$$\begin{aligned}
 p_c(2, N_t, T) = & \frac{\left\{ 4(1+T)^{-1-2N_t} \left( 6(1+T) - (1+T)^{N_t} (10(1+T) \right. \right. \\
 & \left. \left. + \alpha(1+T+N_t T) \right) {}_2F_1 \left[ N_t, -\frac{2}{\alpha}, \frac{-2+\alpha}{\alpha}, -T \right] \right. \\
 & \left. + (4+\alpha)(1+T)^{1+2N_t} {}_2F_1 \left[ N_t, -\frac{2}{\alpha}, \frac{-2+\alpha}{\alpha}, -T \right]^2 \right\}}{\alpha^2 {}_2F_1 \left[ N_t, -\frac{2}{\alpha}, \frac{-2+\alpha}{\alpha}, -T \right]^4} \\
 & + p_c(1, N_t, T). \tag{D.1}
 \end{aligned}$$

The above equation can be used to compute the coverage probability and spectral efficiency when  $N_r = N_t + 2$ .

**D.2. Probability of coverage in coordinated scheduling**

The expression for coverage probability in CS when  $k = 2$  is given below and the equation can be used to compute the coverage probability and spectral efficiency in CS. The probability of coverage when the MU has  $N_r = N_t + 2$  antennas is given by

$$\begin{aligned}
 p_{c_{CS}}(2, N_t, T) = & \left\{ \frac{\left( -(3\Gamma[N_t] - \Gamma[N, TN_t]) \left( 1 + \frac{2T}{N_t} \right)^{-2N_t} \right)}{(\Gamma[N] \Psi(N_t, -2\nu)^4)} \right. \\
 & + \frac{e^{-TN_t} \left( 1 + \frac{2T}{N_t} \right)^{-N_t} (7e^{TN} \Gamma[N_t] - 7e^{TN} \Gamma[N_t, TN_t] - 4(TN_t)^{N_t})}{\Gamma[N] \Psi(N_t, -2\nu)^3} \\
 & \left. + \frac{-4 + \frac{4\Gamma[N_t, TN_t] + 6e^{-TN_t} (TN_t)^{N_t}}{\Gamma[N_t]}}{\Psi(N_t, -2\nu)^2} \right\} \\
 & + 2N_t \left\{ \frac{-\left( 1 + \frac{T}{N_t} \right)^{-N_t}}{\Psi(N_t, -\nu)^3 (T + N_t)} - \frac{\left( 2T \left( 1 + \frac{T}{N_t} \right)^{-N_t} \right)}{\Psi(N_t, -\nu)^3 (T + N_t)} \right\}
 \end{aligned}$$

$$\begin{aligned}
 & + \frac{\left(2T\left(1 + \frac{2T}{N_t}\right)^{-N_t}\right)}{\Psi(N_t, -2\nu)^3(2T + N_t)} + \frac{1}{\Gamma[N_t]} \left(e^{-TN_t}(-1 + T)(TN_t)^{N_t}\right. \\
 & + \frac{e^{-TN_t}(-1 + T)(TN_t)^{N_t}}{\Psi(N_t, -\nu)^2} - \frac{2e^{-TN_t}(-1 + T)(TN_t)^{N_t}}{\Psi(N_t, -\nu)^2} \\
 & \left. + \frac{(1 + 2T)\Gamma[N_t, TN_t]\left(1 + \frac{T}{N_t}\right)^{-N_t}}{\Psi(N_t, -\nu)^3(T + N_t)} - \frac{2T\Gamma[N_t, TN_t]\left(1 + \frac{2T}{N_t}\right)^{-N_t}}{\Psi(N_t, -2\nu)^3(2T + N_t)}\right) \Bigg\} \\
 & + \frac{1}{\Gamma[N_t]} 2 \left\{ \frac{3(\Gamma[N_t] - \Gamma[N_t, TN_t])\left(1 + \frac{T}{N_t}\right)^{-2N_t}}{\Psi(N_t, -\nu)^4} + e^{-TN_t}(TN_t)^{N_t} \right. \\
 & + \frac{(4\Gamma[N_t] - 4\Gamma[N_t, TN_t] - 6e^{-TN_t}(TN_t)^{N_t})}{\Psi(N_t, -\nu)^2} \\
 & \left. (e^{-TN_t}\left(1 + \frac{T}{N_t}\right)^{-N_t}(N_t(-6e^{TN_t}\Gamma[N_t] + 6e^{TN_t}\Gamma[N_t, TN_t]) \right. \right. \\
 & \left. \left. + 4(TN_t)^{N_t} + T(-7e^{TN_t}\Gamma[N_t] + 7e^{TN_t}\Gamma[N_t, TN_t]) \right. \right. \\
 & \left. \left. + 4(TN_t)^{N_t})\right) \right\} \\
 & + p_{c_{cs}}(1, N_t, T) \tag{D.2}
 \end{aligned}$$

**References**

1. B. Błaszczyszyn and M. K. Kararay, Quality of service in wireless cellular networks subject to log-normal shadowing, *IEEE Trans. Commun.* **61** (2013) 781–791.
2. J. Wu, N. B. Mehta and A. F. Molisch, Unified spectral efficiency analysis of cellular systems with channel-aware schedulers, *IEEE Trans. Commun.* **59** (2011) 3463–3474.
3. G. Nigam, P. Minero and M. Haenggi, Coordinated multipoint joint transmission in heterogeneous networks, *IEEE Trans. Commun.* **62** (2014) 4134–4146.
4. A. Chopra and B. L. Evans, Joint statistics of radio frequency interference in multi-antenna receivers, *IEEE Trans. Signal Process.* **60** (2012) 3588–3603.
5. O. El Ayach, S. Peters and R. W. Heath Jr., The feasibility of interference alignment over measured MIMO-OFDM channels, *IEEE Trans. Vehicular Technol.* **59** (2010) 4309–4321.

6. H. Huang, C. B. Papadias and S. Venkatesan, *MIMO for Cellular Networks* (Springer, New York, 2012).
7. B. Pijcke, M. Zwingelstein-Colin, M. Gazalet, M. Gharbi and P. Corlay, An analytical model for the intercell interference power in the downlink of wireless cellular networks, *EURASIP J. Wireless Commun. Networking* **95** (2011) 1–20.
8. Y. S. Soh, T. Q. S. Quek, M. Kountouris and H. Shin, Energy efficient heterogeneous cellular networks, *IEEE J. Sel. Areas Commun.* **31** (2013) 840–850.
9. J. G. Andrews, F. Baccelli and R. K. Ganti, A tractable approach to coverage and rate in cellular networks, *IEEE Trans. Commun.* **59** (2011) 3122–3134.
10. S. Mukherjee, Distribution of downlink SINR in heterogeneous cellular networks, *IEEE J. Sel. Areas Commun.* **30** (2012) 575–585.
11. H. S. Dhillon, R. K. Ganti, F. Baccelli and J. G. Andrews, Modeling and analysis of K-tier downlink heterogeneous cellular networks, *IEEE J. Sel. Areas Commun.* **30** (2012) 550–560.
12. H.-S. Jo, Y. J. Sang and J. G. Andrews, Heterogeneous cellular networks with flexible cell association: A comprehensive downlink SINR analysis, *IEEE Trans. Wireless Commun.* **11** (2012) 3484–3495.
13. P. Madhusudhanan, J. G. Restrepo, Y. Liu and T. X. Brown, Downlink coverage in a heterogeneous cellular Networks, *Proc. IEEE Global Communications Conference, Anaheim, USA* (2012), pp. 4170–4175.
14. D. Gesbert, S. Hanly, H. Huang, S. S. Shitz, O. Simeone and W. Yu, Multi-cell MIMO cooperative networks: A new look at Interference, *IEEE J. Sel. Areas Commun.* **28** (2010) 1380–1408.
15. S. Akoum and R. Heath Jr., Interference coordination: Random clustering and adaptive limited feedback, *IEEE Trans. Signal Process.* **61** (2013) 1822–1834.
16. L. Xu, D. Xu, X. Zhang, S. Xu and J. Wang, Dynamic resource allocation with finite rate feedback for multiuser MIMO-OFDM systems, *J. Circuits, Sys. Comput.* **20** (2011) 501–513, doi: 10.1142/S0218126611007414.
17. J. Zhang and J. G. Andrews, Adaptive spatial intercell interference cancellation in multicell wireless networks, *IEEE J. Sel. Areas Commun.* **28** (2010) 1455–1468.
18. A. M. Hunter and J. G. Andrews, Transmission capacity of ad-hoc networks with spatial diversity, *IEEE Trans. Wireless Commun.* **7** (2008) 5058–5070.
19. V. Chandrasekhar, M. Kountouris and J. G. Andrews, Coverage in multi-antenna two-tier networks, *IEEE Trans. Wireless Commun.* **8** (2009) 5314–5327.
20. C. Chen, L. Bai, Y. Li, Y. Jin and J. Choi, Multiuser beamforming in multicell downlinks for maximizing worst signal to interference plus noise ratio, *IET Commun.* **7** (2013) 1596–1604.
21. D. N. C. Tse and P. Viswanath, *Fundamentals of Wireless Communications* (Cambridge University Press, New York, 2005).
22. J. Zander and S. L. Kim, *Radio Resource Management for Wireless Networks* (Artech House, Norwood, MA, New York, 2001).
23. 3GPP TR 36.819, Technical Specification Group Radio Access Network, Coordinated multi-point operation for LTE physical layer aspects (Release 11) Version 2.0.0 (2011) pp. 9–16.
24. S. Y. Jung, H.-K. Lee and S.-L. Kim, Worst-Case user analysis in poisson voronoi cells, *IEEE Commun. Lett.* **17** (2013) 1580–1583.
25. S. T. Veetil, K. Kuchi, A. K. Krishnaswamy and R. K. Ganti, Coverage and rate in cellular networks with multi user spatial Multiplexing, *Proc. IEEE Int. Conf. on Communications*, Budapest, Hungary (2013), pp. 5855–5859.

26. H. S. Dhillon, M. Kountouris and J. G. Andrews, Downlink MIMO HetNets: Modeling, ordering results and performance analysis, *IEEE Trans. Wireless Commun.* **12** (2013) 5208–5222.
27. R. W. Heath Jr., M. Kountouris and T. Bai, Modeling heterogeneous interference using poissonpoint processes, *IEEE Trans. Signal Process.* **61** (2013) 4114–4126.
28. L. Muehle, The Poisson–Voronoi tessellation: Relationship for edges, *Adv. Appl. Probab.* **37** (2005) 279–296.
29. Y. Junh, S. Lee and J. Kim, Design and implementation of symbol detector for MIMO spatial multiplexing systems, *J. Circuits, Syst. Comput.* **20** (2011) 727–739, doi: 10.1142/S0218126611007578.
30. I. S. Gradshteyan, I. M. Ryzhik, A. Jeffrey and D. Zwillinger, *Tables of Integrals, Series, and Products*, 6th edn. (Academic Press, San Diego CA, 2000).
31. H. Shirani-Mehr, G. Caire and M. J. Neely, MIMO downlink scheduling with non-perfect channel state knowledge, *IEEE Trans. Commun.* **58** (2010) 2055–2066.
32. R. K. Ganti and K. Kuchi, SINR order statistics in OFDMA systems, *Proc. IEEE Global Communications Conference*, Anaheim, USA (2012), pp. 4159–4164.